



# Hard tissue volumetric and soft tissue contour linear changes at implants with different surface characteristics after experimentally induced peri-implantitis: an experimental in vivo investigation

R. Di Raimondo<sup>1</sup> · Javier Sanz-Esporrin<sup>2,3</sup>  · I. Sanz Martin<sup>1</sup> · F. Vignoletti<sup>2</sup> · J. Nuñez<sup>1</sup> · F. Muñoz<sup>4</sup> · H. J. Haugen<sup>5</sup> · M. Sanz<sup>1,2</sup>

Received: 24 September 2020 / Accepted: 27 November 2020 / Published online: 7 January 2021  
© The Author(s), under exclusive licence to Springer-Verlag GmbH, DE part of Springer Nature 2021

## Abstract

**Objective** To evaluate the hard tissue volumetric and soft tissue contour linear changes in implants with two different implant surface characteristics after a ligature-induced peri-implantitis.

**Material and methods** In eight beagle dogs, implants with the same size and diameter but distinct surface characteristics were placed in the healed mandibular sites. Test implants had an external monolayer of multi-phosphonate molecules (B+), while control implants were identical but without the phosphonate-rich surface. Once the implants were osseointegrated, oral hygiene was interrupted and peri-implantitis was induced by placing subgingival ligatures. After 16 weeks, the ligatures were removed and peri-implantitis progressed spontaneously. Bone to implant contact (BIC) and bone loss (BL) were assessed three-dimensionally with Micro-Ct ( $\mu$ CT). Dental casts were optically scanned and the obtained digitalized standard tessellation language (STL) images were used to assess the soft tissue vertical and horizontal contour linear changes.

**Results** Reduction of the three-dimensional BIC percentage during the induction and progression phases of the experimental peri-implantitis was similar for both the experimental and control implants, without statistically significant differences between them. Soft tissue analysis revealed for both implant groups an increase in horizontal dimension after the induction of peri-implantitis, followed by a decrease after the spontaneous progression period. In the vertical dimension, a soft tissue dehiscence was observed in both groups, being more pronounced at the buccal aspect.

**Conclusions** The added phosphonate-rich surface did not provide a more resistant environment against experimental peri-implantitis, when assessed by the changes in bone volume and soft tissue contours.

**Clinical relevance** Ligature-induced peri-implantitis is a validated model to study the tissue changes occurring during peri-implantitis. It was hypothesized that a stronger osseointegration mediated by the chemical bond of a phosphonate-rich implant surface would develop an environment more resistant to the inflammatory changes occurring after experimental peri-implantitis. These results, however, indicate that the hard and soft tissue destructive changes occurring at both the induction and progression phases of experimental peri-implantitis were not influenced by the quality of osseointegration.

**Keywords** Experimental in vivo investigation · Implant surface microtopography · Experimental peri-implantitis · Micro-CT analysis · Volumetric analysis

✉ Javier Sanz-Esporrin  
javisanzes@gmail.com

<sup>1</sup> Graduate Clinic of Periodontology, Faculty of Odontology, University Complutense, Madrid, Spain

<sup>2</sup> ETEP (Etiology and Therapy of Periodontal and Peri-Implant Diseases) Research Group, University Complutense, Madrid, Spain

<sup>3</sup> Facultad de Odontología, Universidad Complutense de Madrid, Plaza Ramón y Cajal s/n (Ciudad Universitaria), 28040 Madrid, Spain

<sup>4</sup> Department of Veterinary Clinical Sciences, University of Santiago de Compostela, Lugo, Spain

<sup>5</sup> Department of Biomaterials, Institute for Clinical Dentistry, University of Oslo, Oslo, Norway

## Introduction

Oral rehabilitation with dental implants after tooth extraction is the current standard of care, with demonstrated high long-term survival rates (94.6% after 10 years) [1]. However, in spite of these high survival rates, a high incidence of both technical and biological complications has been reported [2]. At the World Workshop of Periodontology, a new classification of peri-implant diseases was introduced [3, 4] defining peri-implantitis as a pathological condition caused by biofilm accumulation on the implant-supported restoration and characterized by inflammation of the peri-implant soft tissues and progressive bone loss [5]. Prevalence of peri-implantitis has been estimated between 15 and 25% at patient level, although these figures vary depending on the different populations assayed, the long-term evaluation, and the threshold of bone level changes used to define the cases [6, 7]. Although this disease shares a similar etiology and pathogenesis with periodontitis, it has shown a more rapid and advanced progression [5, 8, 9]. In its incidence and progression, there are well-established risk factors, such as the patient's history of periodontitis and its oral hygiene practices and lack of compliance with maintenance therapy [5, 10, 11]; however, there are other risk indicators associated with the implant itself and implant site that have not yet been validated in prospective cohort studies [4]. Among them, the possible influence of the implant design, mainly the implant surface topographic characteristics, has been evaluated in recent systematic reviews. Although rougher compared to smoother surfaces seem to favor plaque accumulation and hence peri-implantitis, there is a high discrepancy among the results from different investigations [12, 13].

Different investigators have hypothesized that by changing the chemical composition of the implant surface design, the quality of osseointegration might increase and lead to a stronger higher bone to implant contact (BIC), what might decrease the incidence of peri-implantitis [14]. This was not the case of calcium phosphate coatings that failed to demonstrate a higher degree of osseointegration when compared to standard implant surfaces of pure titanium [15, 16]. The addition of an external layer of multi-phosphonate molecules to the traditional implant surface was designed for increasing the implant wettability and thus favoring a faster osteoblastic activity and a stronger bond between the bone and the implant surface [17, 18]. Histological preclinical *in vivo* investigations showed that this surface modification could accelerate the bone healing process by promoting faster bone formation and osseointegration [19]. Clinically, this multi-phosphonate-coated surface (SurfLink®, Nano Bridging Molecules, Gland, Switzerland) has been evaluated against a standard roughened implant surface, but results did not provide a significant benefit compared with standard implants and the authors suggested that this surface should be tested

under more critical conditions [20]. One of these critical conditions may be to evaluate the resistance of this bioactive surface when exposed to the etiological conditions leading to peri-implantitis. It was therefore the aim of this preclinical *in vivo* investigation to evaluate the behavior of this novel implant surface by assessing the peri-implant hard and soft tissue changes after experimental peri-implantitis using  $\mu$ CT volumetric analysis to assess the bone changes and digitalized standard tessellation language (STL) images to assess the soft tissue contour lineal changes.

## Material and methods

### Study design

This preclinical *in vivo* investigation was designed according to the modified ARRIVE guidelines [21]. The protocol of this investigation was approved by the Regional Ethics Committee for Animal Research of the University of Santiago de Compostela (Ref. AE-LU-001/04/16) assuring the compliance with the Spanish regulation RD53/2013 for preclinical investigations, including the handling, physiological conditions, health care, nutrition, and housing of the experimental animals used in the investigation.

All surgical procedures and soft tissue contour linear changes analysis were performed at the Department of Veterinary, in the University of Lugo, Spain. The  $\mu$ CT data acquisition and 3D hard tissue volumetric analysis were performed in the Department of Biomaterials, University of Oslo.

The study population consisted of eight female adult Beagle dogs acquired from the Service of Animal Experimentation of the University of Cordoba, Spain, with a mean age of 72 months, weighting between 12 and 15 kg. Each experimental animal was maintained in individual kennels in a 12:12 light/dark cycle and 22–21 °C and monitored daily by an experienced veterinarian, being each identified with a subcutaneous chip code that remained during the entire follow-up of the study. Food was based on soft pallet diet and the animals had free access to water. Before final inclusion for the investigation, all animals were observed 2 weeks prior to the surgical procedures to assure their general health status.

### Surgical interventions

All surgical procedures were carried out between June 2016 and July 2017. The study could be divided in three different time periods: (a) the preparatory phase (from June and November 2016); (b) the induction period of peri-implantitis (from November 2016 and February 2017); and (c) the spontaneous progression of peri-implantitis until euthanasia (from February and July 2017).

Immediately before each surgery, the animals were sedated with propofol (2 mg/kg/i.v., Propovet, Abbott Laboratories, Kent, UK) and placed under general anesthesia with 2.5–4% of isoflurane (Isoba-vet, Schering-Plough, Madrid Spain) for the entire period of the surgery. Lidocaine 2% with epinephrine 1:100.000 (2% Xylocaine Dental, Dentsply, York, PA, USA) was also infiltrated locally to reduce intra-operative bleeding. The preparatory phase included two different periods of 3 months each. In the first surgery, the second, third, and fourth lower premolars (P2, P3, P4) and the first molar (M1) were extracted once hemisected (Fig. 1a) (Fig. 1b). The extraction sockets were left to heal spontaneously during 3 months, during which time the oral hygiene of the dogs was maintained professionally, using soft toothbrushes and toothpaste, and by applying a gauze impregnated with a Chlorhexidine solution (0.12%), three times per week.

After this period, the second surgery consisted in the elevation of full thickness flaps to expose the healed edentulous ridges (Fig. 1c), and the placement of ten implants, five in each hemi-mandible; all had identical geometry (9 mm (mm) long and 3.5 mm in diameter ( $\emptyset$ )) but with two different surface characteristics. Randomization of the interventions

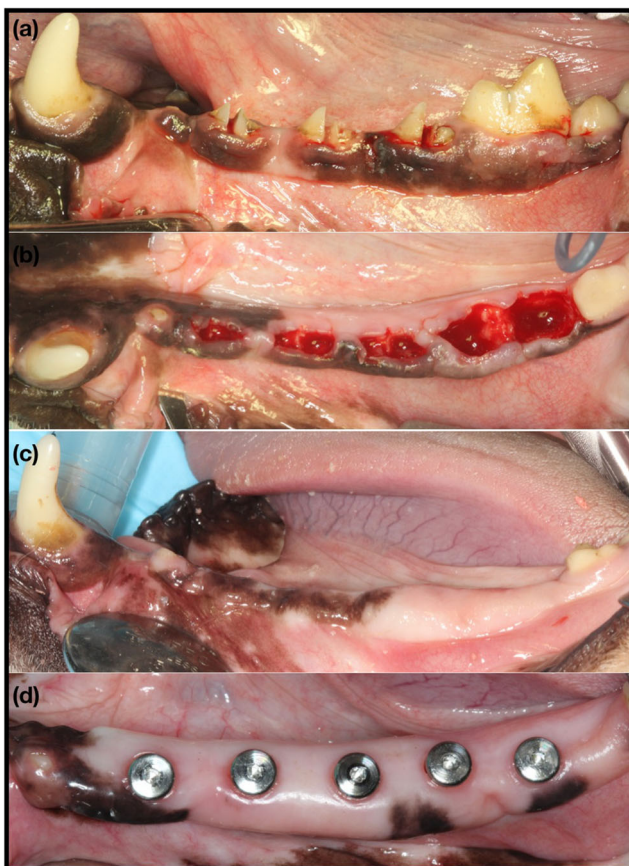


**Fig. 1** Images of the experimental surgeries. Preparatory phase. **a** Hemisection of P2, P3, P4, and M1. **b** Extractions of P2, P3, P4, and M1. **c** Healed ridge crest after 3 months from the extractions. **d** Implant placement before induced peri-implantitis

was performed using a computer-generated block randomization list (IBM SPSS Statistics® V20 JM.Domenech) that considered the type and position of each implant in the jaw, as well as the type of implant (test and control) placed in each hemi-mandible.

Both test and control implants were made of titanium grade 5 following the C1 design (MIS® Dental Implants, Israel) with a customized reduced diameter of 3.5 mm with an internal hexagon connection and with a moderately rough surface obtained by sand blasting and acid etching. Without altering the micro and macro characteristics of the topography, the test implants received a monomolecular layer of multi-phosphonate (SurfLink®, Nano Bridging Molecules, Gland, Switzerland). Control implants were identical, but without the monomolecular layer of multi-phosphonate. Once the implants were placed, healing abutments of 4.5 mm in diameter were secured and the flaps were closed with absorbable sutures (Vicryl® 4.0, Johnson & Johnson, Sint-Stevens-Woluwe, Belgium). Sutures were removed after 14 days and oral hygiene was maintained for the period of the osseointegration of the implants (3 months) (Fig. 1d).

After this period, the induction of peri-implantitis started, by interrupting the oral hygiene regime, and by placing silk ligatures in a subgingival position around the neck of each implant, as previously described by Lindhe [22] (Fig. 2a). Every 4 weeks for 4 months, all ligatures were replaced to allow for the apical progression of peri-implantitis. After this period, the ligatures were removed (Fig. 2b) and during 4 months, no oral hygiene was provided and dental plaque was allowed to accumulate (spontaneous progression phase) (Fig. 2c). In summary, the experimental phase of this investigation included 8 study visits, the first two belonging to the preparatory phase, four visits where ligatures were monthly placed and replaced (induction phase of the peri-implantitis), and the last two visits without ligatures and oral hygiene (spontaneous progression).

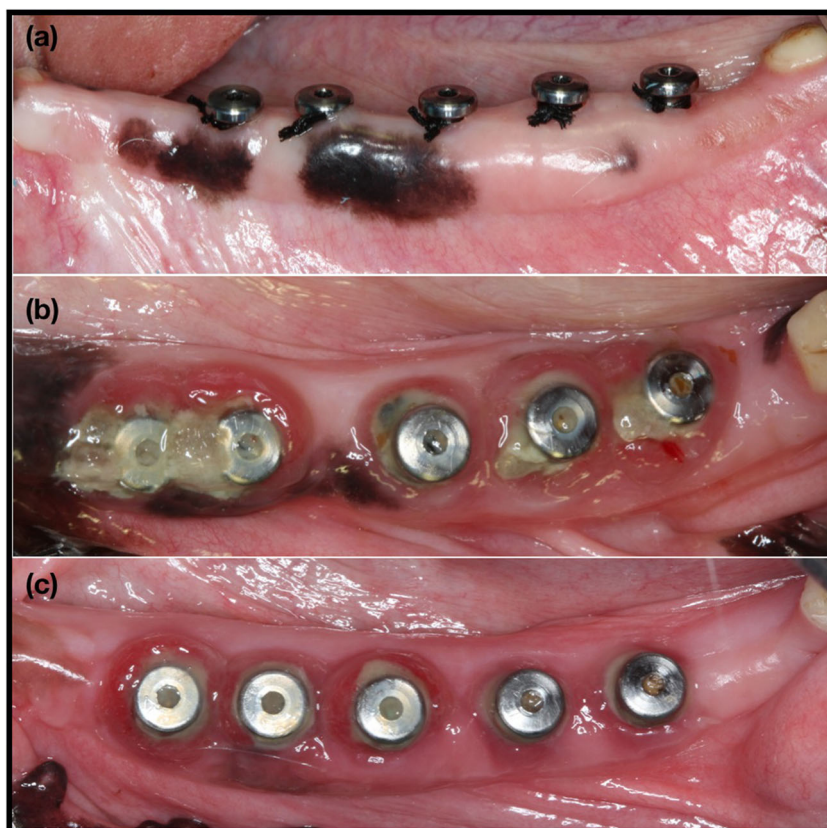
After this period, the animals were euthanized using a lethal dose of sodium Pentothal (40–60 mg/kg/i.v., Dolethal, Vetoquinol, France) and the mandibles were dissected: half of the specimens were processed for non-decalcified histological analysis, and the other half for decalcified soft tissue histological analysis. In this last group, the volumetric hard tissue changes were analyzed by  $\mu$ CT before the histological processing. The histological outcomes of this investigation have been presented in an independent report.

### Volumetric hard tissue analysis: $\mu$ CT image acquisition and data analysis

All specimens were scanned before being sectioned using a high-resolution multi-scale Nano-CT (Skyscan 2211, Bruker microCT NV, Kontich, Belgium) (Fig. 3a). The X-ray source was set at 80 Kv and 90  $\mu$ A with a voxel size of 20  $\mu$ m and a



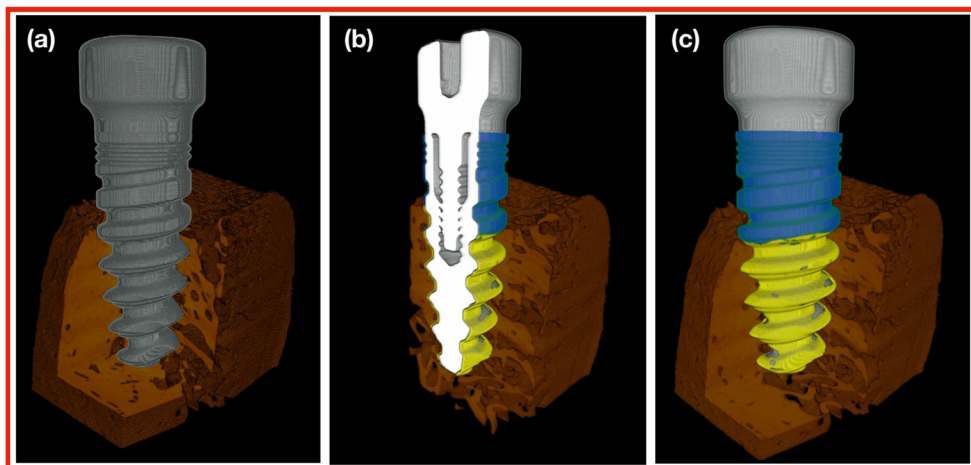
**Fig. 2** Images of the experimental peri-implantitis model. **a** Placement of ligatures around each implant. **b** Peri-implant tissues after the induction of peri-implantitis with subgingival ligatures. **c** Peri-implant tissues after the spontaneous progression of peri-implantitis once the ligatures were removed



0.5-mm titanium filter. The scanning was performed over a 360° rotation, acquiring images every 0.3°. Once scanned, images were reconstructed using the Feldkamp algorithm [23] and NRecon software (Bruker microCT NV, Kontich, Belgium). The reconstructed images were evaluated with the Data Viewer software (Bruker microCT NV, Kontich, Belgium) and rotated to ensure that the implant was perfectly aligned. Both the image acquisition and the hard tissue analysis were performed by the same investigator (JSE), following a training of 3 months in the Department of Biomaterials, at the University of Oslo. A volume of interest (VOI) of 4 to

6 mm of diameter was selected manually in each specimen from the implant shoulder to first bone to implant contact (VOI) to assess peri-implant bone loss (BL). In this VOI, the images were segmented and using global thresholding methods, the best threshold parameters for bone and for implant were set. Then, by measuring the implant surface free of bone contact, the bone loss was calculated. A second VOI, from the first bone to implant contact to the implant apex, was selected to assess the total volume of osseointegration. This was done by measuring the intersecting surface between the bone and the implant (BIC) using the method described by

**Fig. 3** Images of the hard tissue analysis with Micro-Ct. **a** Implant section before the analysis. **b** Cross-sectional section that divides the implant into two equal parts. Blue area represents implant surface that has lost bone support. Yellow area represents tridimensional bone to implant contact. **c** Tridimensional implant section used for the analysis; Blue area represents tridimensional bone loss (BL), while yellow area represents tridimensional bone to implant contact (BIC)



Bruker (method note 074, “Osteointegration: analysis of bone around a metal implant” 2015). To perform the analysis, the three-dimensional area comprised between the platform (coronal) and the apex of the implant was considered the 100% of the volume around implants. Both parameters, bone to implant contact (BIC) and bone loss (BL), were reported as percentage (%) of the total volume around implants and were expressed in cubic millimeters ( $\text{mm}^3$ ) (Fig. 3b) (Fig. 3c). Micro-CT data analysis was performed using the CTAn software (Bruker microCT NV, Kontig, Belgium).

### Soft tissue contour analysis: STL image and data analysis

Individual trays were fabricated for each dog from dental impressions made before tooth extractions. Then, mandibular impressions using a light/heavy silicon (Elite HD +, Zhermack spa, RO, Italy) were obtained, (1) after implant placement and before the placement of ligatures (T1), (2) after the ligatures were removed (T2), and (3) before the sacrifice of the animals (T3) (Fig. 4a) (Fig. 4b) (Fig. 4c). These impressions were poured in dental stone (Fujirock type 4, GC, Corp, Tokyo, Japan) and once the obtained cast models were evaluated to detect possible imperfections or irregularities of the stone, they were scanned with a desktop 3D scanner (Zfx Evolution Scanner, Zimmer Dental, Bolzano, Italy) to obtain standard tessellation language (STL) images (Fig. 4d) (Fig. 4e). These STL files were analyzed by superimposing (matching) the subsequent images using the dedicated software SMOP (Swissmeda Software, Swissmeda AG, Zurich, Switzerland). To obtain a correct matching, three to five fixed reference points (the anterior teeth and the healing abutments, which were not changed during the investigation) were selected at the baseline and at the subsequent follow-up models, then the software performed automatically a “rough fit” superimposition. Then, further points of reference (no less than 10 points) were selected manually, until the software achieved a “fine fit” superimposition based on a series of mathematical algorithms [24]. Using the superimposed images, the soft tissue contour linear changes were measured by a trained investigator (RDR) using the method previously described by this research group [25, 26]. In brief, the method consists of drawing a longitudinal buco-lingual slice at the level of each implant obtaining a cross-sectional section that divides each implant in two halves (Fig. 5a). Then, a vertical line was drawn coinciding with the center of the healing abutment and the axis of the implant (Fig. 5b). The soft tissue changes were calculated by measuring the linear changes in both the horizontal (contour) and vertical dimensions (changes in the position of gingival margin (GM)) with an image analysis software (OLYMPUS® cellSens Dimension Desktop 1.14).

To assess the contour changes, perpendicular lines were drawn at 1, 2, 3, 4, and 5 millimeters (mm) from the GM on

the baseline models. These horizontal lines crossed both the lingual and the buccal contours of the crest. Similarly, to assess the vertical changes, vertical lines were drawn from the GM of the three superimposed STL to the top of the healing abutment, at both the lingual and buccal aspects. We assigned negative values when the linear contours increased (clinically revealing inflamed soft tissues), while positive values were assigned when the soft tissue contours diminished (clinically revealing a loss of tissue). Similarly, vertical measurements were expressed as positive values when the GM moved apically (clinically revealing a soft tissue dehiscence), while negative values corresponded to a coronal displacement of the position of the GM (clinically revealing inflamed soft tissues).

Three different comparisons were done by subtracting the linear measurements of the models taken at different time points (between T1 and T2 (induction period of peri-implantitis), between T2 and T3 (spontaneous progression of peri-implantitis), and between T1 and T3 (changes throughout the investigation) (Fig. 5c).

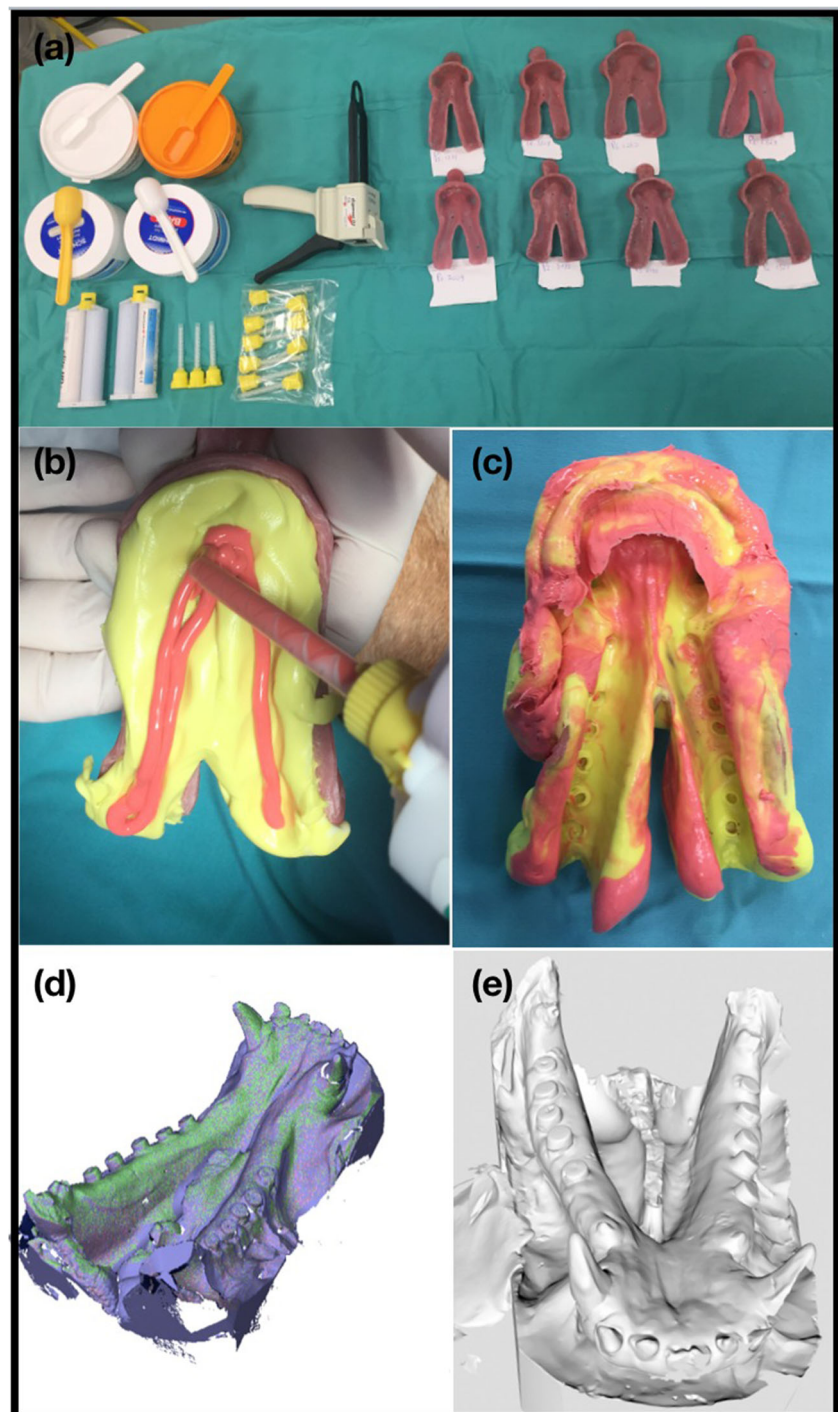
### Data analysis

The dog was considered the unit of all the analysis. The hard tissue volumetric analysis ( $\mu\text{CT}$ ) was evaluated at the end of the investigation after retrieving the specimens before their decalcification.  $\mu\text{CT}$  data were expressed as means, standard deviation (SD), and confidence intervals. The soft tissue contour linear analysis was calculated at three different time points (T1, T2, T3) and data were also expressed as means, standard deviation (SD), and confidence intervals. Shapiro-Wilk normality tests were performed to assess the data distribution. *T* tests were used for the inter-group comparisons, while ANOVA tests were used to compare the differences of the contour linear measurements in terms of height (vertical) and width (horizontal). Bonferroni corrections were performed for multiple comparisons. The alpha error was set at 0.05.

### Results

Healing after all the surgical procedures was uneventful in all the experimental animals, and no implants were lost during the study. Soft and hard tissue analyses were performed in all the dogs, but not in all the implants. Among the 80 implants placed, the most mesially placed in each hemi-mandible were not included in the analysis, since in these implants a dehiscence defect was surgically to test a hypothesis not studied in the present investigation. From the remaining 64 implants,  $\mu\text{CT}$  volumetric analysis was carried out for 32 implants (16 test and 16 control) and soft tissue contour linear changes for 47 implants (24 test and 23 control). Seventeen implants (8 test and 9 control) were

**Fig. 4** Images of the impressions and stereolithography (STL) image acquisition. **a** Individual impression trays of each dog and impression materials. **b** Placement of both light and heavy putty silicon inside the individual tray. **c** Impression of the mandible. **d** Cast model during scan process with the extraoral scanner. **e** Acquisition of the STL file



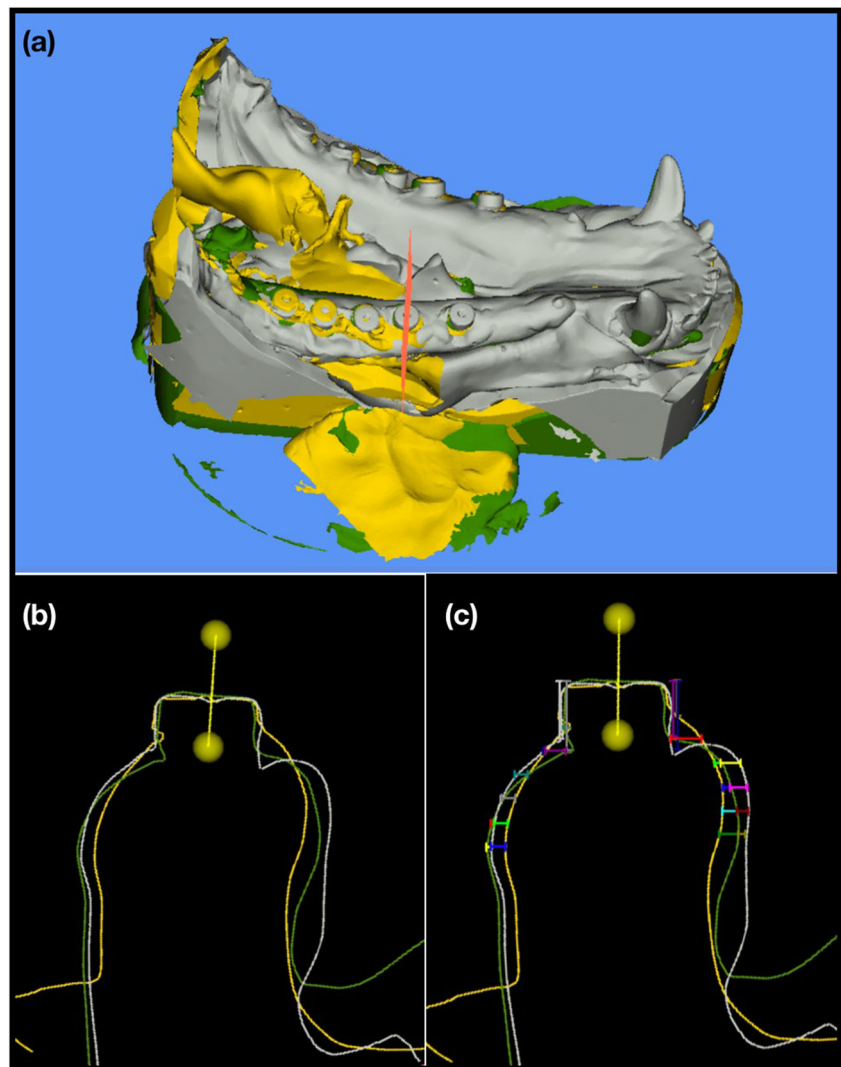
excluded due to the presence of imperfections in the cast models, which made impossible a correct matching of the STL files. The soft tissue analysis resulted in 36 measurements per-each combination of the three superimposed STLs, which corresponded to a total of 1692 linear measurements for the 47 implants considered for the soft tissue analysis, 1410 being horizontal (705 buccal and 705 lingual) and 282 verticals (141 buccal and 141 lingual).

#### Hard tissue $\mu$ CT analysis

Detailed description of the  $\mu$ CT data is depicted in Table 1. Test implants lost more bone than control implants at the end of the experimental peri-implantitis ( $42.94 \text{ mm}^3$  vs  $37.86 \text{ mm}^3$ , respectively), although these differences were not statistically significant ( $p = 0.165$ ). The percentage of total BIC was similar between both implant groups, being slightly



**Fig. 5** Images of the soft tissue analysis. **a** STL files matching of the entire mandible at the three different time points of the study. Red line corresponds to the cross-sectional section that divides the implant into two equal parts. **b** STL files matching at implant level. **c** Vertical and horizontal linear measurements between the different time points of the study at both lingual and buccal aspects. Yellow line represents pre ligatures contour (baseline); green line represents post-ligatures contour; gray line represents post-spontaneous progression contour



higher in the control group when compared with the test group (53.98 mm<sup>3</sup> vs 49.82 mm<sup>3</sup>, respectively) ( $p = 0.132$ ). Both implants lost around 40% of their peri-implant bone support due to peri-implantitis (Supplementary graph 1).

**Soft tissue linear measurements**

Horizontal measurements were drawn at 1, 2, 3, 4, and 5 mm from the GM of the baseline models (T1), thus obtaining 10 measurements (5 buccal and 5 lingual) for each implant, with

a total of 30 measurements for the three time points of the study (induction, spontaneous progression, and begin-end). Table 2 depicts the inter-group comparisons of these horizontal buccal measurements. Differences between test and control implants were not statistically significant, irrespective of the measurement level and the healing periods. During the induction period, positive values were recorded for both groups in the most coronal levels (1 and 2 mm) of the buccal soft tissue contour, revealing a loss of soft tissue, whereas negative values were observed more apically at 3, 4, and 5 mm,

**Table 1** Micro-Ct volumetric data of hard tissue. All measurements are expressed in cubic millimeters

Measurements	Mean (SD) C group	IC 95% (Inf. Lim; Sup. Lim)	Mean (SD) T group	IC 95% (Inf. Lim; Sup. Lim)	Mean Δ C/T	IC 95% (Inf. Lim; Sup. Lim)	<i>p</i>
% BIC 360	53.98 (5.21)	49.62; 58.35	49.82 (4.64)	45.53; 54.12	4.15	- 1.38; 9.70	0.132
% Bone loss	37.86 (6.48)	32.44; 43.28	42.94 (3.72)	39.49; 46.38	- 5.07	- 11.09; 0.94	0.165

*SD*, standard deviation; *IC 95%*, confidence interval 95%;  $\Delta$ , mean difference; *T*, test group; *C*, control group; *BIC*, bone to implant contact

**Table 2** Prophilometric linear changes of soft tissue at buccal aspect. Inter-group comparisons. All measurements are expressed in millimeters

Period	Measurements	Mean (SD) T group	IC 95% (Inf. Lim; Sup. Lim)	Mean (SD) C group	IC 95% (Inf. Lim; Sup. Lim)	Mean Δ T/C	IC 95% (Inf. Lim; Sup. Lim)	<i>p</i>
Induction	1 mm	0.58 (0.64)	0.04; 1.13	0.65 (0.49)	0.24; 1.06	-0.07	-0.68; 0.54	0.793
	2 mm	0.04 (0.61)	-0.47; 0.55	0.32 (0.64)	-0.20; 0.86	-0.28	-0.96; 0.38	0.294
	3 mm	-0.21 (0.66)	-0.77; 0.33	-0.08 (0.67)	-0.65; 0.47	-0.12	-0.84; 0.58	0.674
	4 mm	-0.24 (0.84)	-0.95; 0.46	-0.30 (0.74)	-0.92; 0.32	0.05	-0.80; 0.90	1.000
	5 mm	-0.42 (1.07)	-1.45; 0.68	-0.61 (0.92)	-1.38; 0.16	0.18	-0.89; 1.25	0.753
Progression	1 mm	-0.05 (0.47)	-0.45; 0.34	0.09 (0.45)	-0.27; 0.47	-0.15	-0.65; 0.34	0.401
	2 mm	0.05 (0.59)	-0.44; 0.55	-0.28 (0.51)	-0.71; 0.14	0.33	-0.25; 0.93	0.345
	3 mm	0.29 (0.55)	-0.16; 0.75	-0.05 (0.37)	-0.36; 0.25	0.34	-0.15; 0.84	0.115
	4 mm	0.35 (0.35)	0.06; 0.65	0.06 (0.40)	-0.27; 0.40	0.28	-0.12; 0.69	0.248
	5 mm	0.46 (0.29)	0.19; 0.73	0.41 (0.67)	-0.14; 0.98	0.04	-0.55; 0.63	0.355
Begin-End	1 mm	0.41 (0.37)	0.10; 0.73	0.59 (0.70)	0.009; 1.18	-0.18	-0.78; 0.42	0.294
	2 mm	0.11 (0.41)	-0.23; 0.46	0.07 (0.71)	-0.52; 0.66	0.04	-0.58; 0.67	0.916
	3 mm	-0.06 (0.48)	-0.46; 0.34	-0.12 (0.50)	-0.54; 0.30	0.06	-0.46; 0.59	0.793
	4 mm	0.005 (0.90)	-0.75; 0.76	-0.16 (0.41)	-0.51; 0.18	0.17	-0.58; 0.92	0.753
	5 mm	0.13 (1.07)	-0.86; 1.12	-0.19 (0.41)	-0.54; 0.14	0.33	-0.55; 1.21	0.817

*SD*, standard deviation; *IC 95%*, confidence interval 95%;  $\Delta$ , mean difference; *T*, test group; *C*, control group

revealing an increase in soft tissue contour. During the progression period, once ligatures were removed, the loss of soft tissue contours continued, irrespective of the groups. When assessing the period between baseline and the end of the study, soft tissue contour increase was only observed at 3 mm for test groups, whereas a similar increase was noted in control groups at the middle and apical levels (3, 4, and 5 mm) (Fig. 6).

Table 3 depicts the inter-group comparisons of the horizontal lingual measurements. Similar to the buccal changes, differences between test and control implants were not statistically significant. During the induction period, increase in soft tissue contours was observed in both groups, revealing an inflamed lingual soft tissue, except in the coronal aspect (1 mm for test group and 1 and 2 mm for control group, respectively) where loss of contour was noted. During the

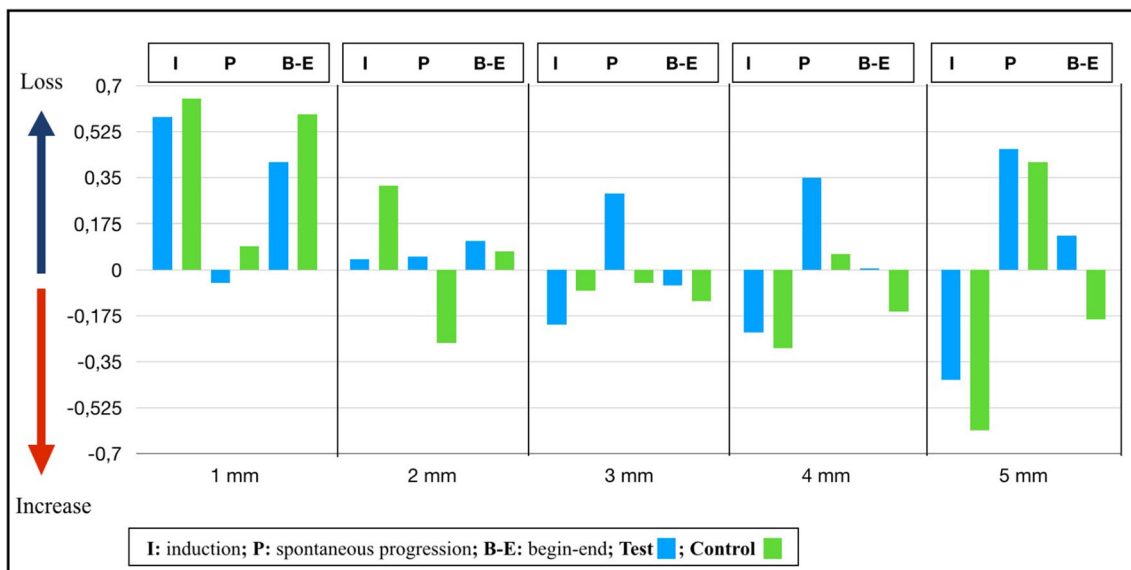


**Fig. 6** Graphic representation of the horizontal buccal contour changes of soft tissue between the different time points of the study (induction, progression, and begin-end) at five different crestal levels (1 mm,

2 mm, 3 mm, 4 mm, 5 mm). Blue and green rectangles corresponded to test and control groups, respectively



**Table 3** Prophilometric linear changes of soft tissue at lingual aspect. Inter-group comparisons. All measurements are expressed in millimeters

Period	Measurements	Mean (SD) T group	IC 95% (Inf. Lim; Sup. Lim)	Mean (SD) C group	IC 95% (Inf. Lim; Sup. Lim)	Mean Δ T/C	IC 95% (Inf. Lim; Sup. Lim)	<i>p</i>
Induction	1 mm	0.49 (0.70)	-0.53; 0.63	0.13 (0.87)	-0.59; 0.86	-0.08	-0.93; 0.76	0.674
	2 mm	-0.25 (0.44)	-0.63; 0.11	0.05 (0.69)	-0.52; 0.64	-0.31	-0.94; 0.30	0.462
	3 mm	-0.44 (0.44)	-0.81; -0.06	-0.14 (0.44)	-0.51; 0.22	-0.29	-0.77; 0.18	0.115
	4 mm	-0.41 (0.45)	-0.79; -0.02	-0.14 (0.39)	-0.46; 0.18	-0.26	-0.72; 0.18	0.115
	5 mm	-0.38 (0.42)	-0.74; -0.03	-0.09 (0.41)	-0.43; 0.25	-0.29	-0.74; 0.15	0.115
Progression	1 mm	0.30 (0.57)	-0.17; 0.79	0.47 (0.42)	0.11; 0.83	-0.16	-0.71; 0.38	0.529
	2 mm	0.52 (0.48)	0.12; 0.92	0.52 (0.40)	0.18; 0.85	0.003	-0.47; 0.47	0.875
	3 mm	0.48 (0.45)	0.10; 0.87	0.38 (0.28)	0.14; 0.62	0.09	-0.30; 0.50	0.401
	4 mm	0.39 (0.53)	-0.04; 0.84	0.26 (0.26)	0.04; 0.48	0.13	-0.31; 0.58	0.529
	5 mm	0.39 (0.53)	-0.04; 0.84	0.17 (0.29)	-0.06; 0.42	0.22	-0.23; 0.68	0.248
Begin-End	1 mm	0.35 (0.50)	-0.06; 0.77	0.60 (0.87)	-0.12; 1.34	-0.25	-1.02; 0.51	0.401
	2 mm	0.26 (0.51)	-0.16; 0.69	0.51 (0.79)	-0.15; 1.17	-0.24	-0.95; 0.46	0.674
	3 mm	0.04 (0.45)	-0.33; 0.42	0.24 (0.54)	-0.21; 0.69	-0.19	-0.73; 0.34	0.563
	4 mm	0.01 (0.39)	-0.31; 0.35	0.12 (0.55)	-0.34; 0.59	-0.10	-0.62; 0.41	0.916
	5 mm	0.01 (0.36)	-0.29; 0.32	0.08 (0.62)	-0.43; 0.60	-0.07	-0.61; 0.47	0.529

*SD*, standard deviation; *IC 95%*, confidence interval 95%;  $\Delta$ , mean difference; *T*, test group; *C*, control group

spontaneous progression period, loss of soft tissue contour occurred in both groups. When comparing baseline with the end of the study, the lingual soft tissue contour also diminished, irrespective of the groups, although a higher loss was noted in the lingual soft tissue contour in the control group (Fig. 7).

Table 4 depicts the inter-group comparisons of the vertical soft tissue linear measurements at both the buccal and lingual mucosal margins during the different study intervals.

Differences between groups were not significant, neither at buccal nor at lingual aspects. Throughout the study, the position of soft tissue margin moved apically, except the time point just after the progression period where a coronal displacement of buccal soft tissue margin was observed for both groups. While test implants presented a higher incidence of buccal soft tissue dehiscence after the induction period and between the baseline and the end of the study compared to control implants, lingual soft tissue dehiscence was more

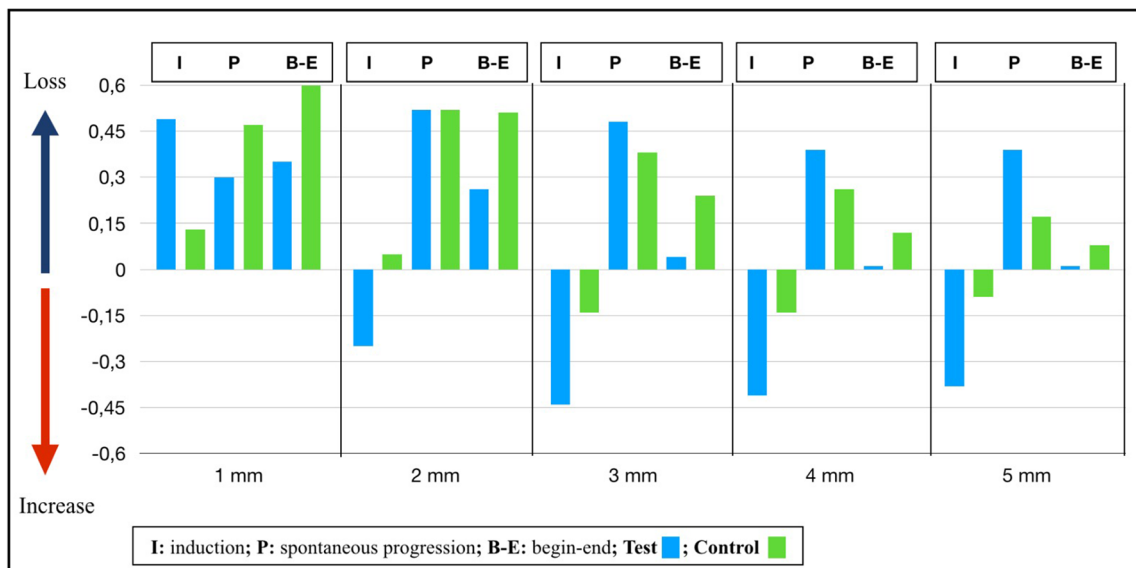


**Fig. 7** Graphic representation of the horizontal lingual contour changes of soft tissue between the different time points of the study (induction, progression, and begin-end) at five different crestal levels (1 mm, 2 mm,

3 mm, 4 mm, 5 mm). Blue and green rectangles corresponded to test and control groups, respectively

**Table 4** Vertical linear changes of soft tissue at both buccal and lingual aspect. Inter-group comparisons. All measurements are expressed in millimeters

Period	Measurements THA-GM	Mean $\Delta$ (SD) T group	IC 95% (Inf. Lim; Sup. Lim)	Mean $\Delta$ (SD) C group	IC 95% (Inf. Lim; Sup. Lim)	Mean $\Delta$ T/C	IC 95% (Inf. Lim; Sup. Lim)	<i>p</i>
Induction	Buccal	1.26 (0.47)	0.86; 1.65	1.12 (0.60)	0.62; 1.63	0.13	-0.45; 0.71	0.834
	Lingual	0.31 (0.89)	-0.43; 1.06	0.46 (0.65)	-0.07; 1.01	-0.15	-0.99; 0.68	0.753
Mean $\Delta$ Buccal-Lingual ( <i>p</i> value)	0.95 (0.004)***			0.66 (0.004)***				
Progression	Buccal	-0.33 (0.42)	-0.69; 0.01	-0.33 (0.38)	-0.66; -0.01	-0.004	-0.44; 0.43	0.958
	Lingual	0.05 (0.45)	-0.32; 0.43	0.33 (0.43)	-0.02; 0.69	-0.28	-0.75; 0.19	0.208
Mean $\Delta$ Buccal-Lingual ( <i>p</i> value)	-0.39 (0.078)			-0.66 (0.004)***				
Begin-End	Buccal	0.92 (0.61)	0.41; 1.43	0.79 (0.64)	0.25; 1.33	0.12	-0.54; 0.80	0.916
	Lingual	0.36 (0.50)	-0.06; 0.78	0.80 (0.69)	0.22; 1.38	-0.43	-1.09; 0.21	0.227
Mean $\Delta$ Buccal-Lingual ( <i>p</i> value)	0.55 (0.003)***			-0.008 (0.930)				

*SD*, standard deviation; *IC 95%*, confidence interval 95%; *THA-GM*, top of healing abutment (THA) and gingival margin (GM)  $\Delta$ , mean difference; *T*, test group; *C*, control group

\*\*\*Statistical significant differences ( $p < 0.05$ )

pronounced in the control group at every time point. When comparing changes in vertical soft tissue contour between the buccal and lingual aspect, it was observed that during the induction period, the buccal soft tissue contour receded 0.95 mm in comparison with the lingual contour in test and 0.66 mm in control implants, respectively. These differences between buccal and lingual contour reduction were statistically significant ( $p = 0.004$ ). During the progression phase, more vertical reduction of the soft tissue contours was observed at the lingual aspect compared with the buccal aspect, in both test (0.39 mm) and control implants (0.66 mm). Differences between buccal and lingual contour reduction were statistically significant only in the control group ( $p = 0.004$ ). When considering vertical contour modification on the complete experimental period (Baseline-End), the buccal soft tissue contour was reduced 0.55 mm more than the lingual contour only in the test group ( $p = 0.003$ ), while in the control group, both lingual and buccal had similar amount of contour reduction (Fig. 8).

## Discussion

This preclinical in vivo investigation has used a novel technology to assess the hard and soft tissue changes occurring during and after experimental peri-implantitis with the goal of comparing two implants with identical micro and macro topographical design, but having the tested implants a

unique bioactive external surface layer of multi-phosphonate molecules, which has shown an increased osseointegration velocity in preclinical studies. The study hypothesis was based in the assumption that a more rapid osseointegration would implicate a harder resistance to deosseointegration, when implants were exposed to a well-validated ligature-induced peri-implantitis model. The deosseointegrated dynamics were evaluated at two levels, first by assessing the net 360° bone loss and bone to implant contact using  $\mu$ CT scans, and second by measuring the changes of the soft tissue linear contours, both buccally and lingually resulting from the induction and progression phases of ligature-induced peri-implantitis. The  $\mu$ CT data indicated that a pronounced bone loss occurred after peri-implantitis induction and progression for both test and control implants. Even though more bone loss occurred for the test implants, these differences were not statistically significant when compared with the control implants. The results on the soft tissue linear changes showed that during the induction period, there was a horizontal increase of soft tissue contours, while during the spontaneous progression, these soft tissue contours receded. Again, differences between test and control implants were not statistically significant, at both the buccal and lingual sides. In vertical dimension, a soft tissue dehiscence was observed for both groups, being more pronounced at the buccal aspect after the induction period. No significant differences were observed between the test and control implants.

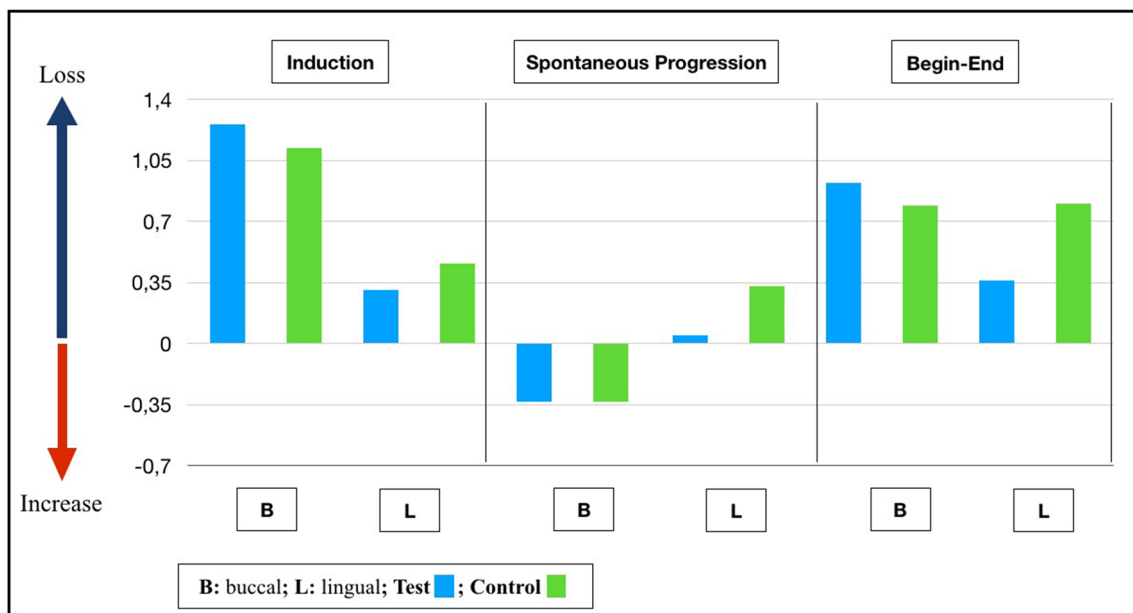


**Fig. 8** Graphic representation of the vertical buccal and lingual contour changes of test and control groups between the different moments of the study (induction, progression, and begin-end. Blue and green rectangles corresponded to test and control groups, respectively

The increase in soft tissue contour reported in both implant surfaces during the induction period may be explained, mainly by the severe inflammatory reaction resulting from the placement of the ligatures. Additionally, the submarginal placement of the ligatures may also increase the marginal tissue contours. During the progression phase, the reported reduction in tissue contours in both test and control implants may be explained by first, the removal of the ligatures, which reduced the marginal contours, and second, by the resulting tissue loss as a consequence of the inflammation decrease and the net tissue loss, what resulted in a marked recession.

The differential microscopic design of the tested implants was characterized by a hydrophilic surface that consisted of a monomolecular layer of multi-phosphonates covalently bound to the implant surface. This implant surface was previously tested in a preclinical investigation in sheep, evaluating as outcome the quality of osseointegration using histology, histomorphometry, and scanning electron microscopy [19]. The results from that investigation showed higher removal torque values and higher BIC percentages in implants with this new hydrophilic surface compared with similar implants without it, mainly during the first 8 weeks after implant placement, although higher BIC values were maintained up to 52 weeks. These results prompted the authors to define this novel implant surface as osteoconductive, since more woven bone matrix was observed on the tested implant surface, especially during the early healing time [19]. Since in the present investigation the 360° BIC values were calculated once the peri-implantitis was induced, we cannot verify or refute this potential osteoinductivity, nor the increased pace of osseointegration, but clearly shows that once osseointegrated,

these implants were similarly subject to de-osseointegration after peri-implantitis induction, when compared with implants of identical design, but without the hydrophilic surface. In another in vivo investigation using a similar peri-implantitis model and testing two implant surfaces characterized by silver electrodeposition and 3-(triethoxysilyl) propyl succinic anhydride (TEPSA) silane, compared to non-modified implants, the  $\mu$ CT results also did not report significant differences between groups, even though significant differences were described at the histological level [27].

Implants with the multi-phosphonate surface layer were tested also in a randomized clinical trial (RCT) in humans, in both the mandibles and maxilla [20]. No implant failures and no differences in peri-implant mucosal inflammation were observed in both test and control implants during the entire follow-up (12 months). However, after 3 and 12 months from implant loading, less marginal bone loss (MBL) was observed for implants with the treated surface when compared to those without it, although differences were not statistically significant. This study showed that the tested surface was safe but did not provide any significant added benefit over control implants. The authors stated that more studies under more critical conditions were needed [20]. The results from this clinical investigation were confirmed with the results from the present study, since the tested surface did not provide an added value in the prevention of the hard tissue changes associated with peri-implantitis.

In the present study, we have utilized a novel approach to measure the soft tissue contour changes associated with the development of peri-implantitis. The obtained results are in line with the  $\mu$ CT data since no significant differences were



found between the test and control implants. During the active induction period of peri-implantitis predominated the inflammatory component, characterized by a horizontal increase in the contour both at lingual and buccal sides, irrespective of the groups. During this period, soft tissue dehiscence defects developed mainly buccally, what may be explained by the ligatures, whose knots were predominantly tied buccally. Similarly, there were no significant differences between the tested implants and the controls.

During the disease spontaneous progression of peri-implantitis, a decrease in the horizontal soft tissue contour was observed at both buccal and lingual aspects, irrespective of the groups. Similarly, further loss in vertical dimension was noted in both groups, what can be explained by the partial resolution of the inflammation resulting from the removal of the ligatures, what translated in a net hard and soft tissue loss. Finally, when comparing soft tissue contour changes from the start to the end of the investigation, there was a clear horizontal loss in soft tissue contours at all heights in the lingual aspect, irrespective of the groups. However, a slight increase was noted at midlevel (3 mm) in the test group and at both middle and apical levels in the control group (3 mm, 4 mm, 5 mm), that confirms that the pronounced bone loss identified by  $\mu$ CT did not fully translate into loss of soft tissue contours. The results obtained in this investigation in terms of soft tissue inflammation and bone loss during ligature-induced peri-implantitis are similar to those reported in other preclinical studies using the same experimental model [28–32], although the main difference with these studies is the novel methodology used in this investigation to assess the bone volumetric and soft tissue contour changes.

The use of Micro-Ct to measure peri-implant bone changes has shown to be a useful and precise tool to quantify bone density and to measure its volume and microarchitecture, particularly at the trabecular level [33, 34]. Even though most of the investigations have used Micro-Ct to assess bone volume changes after regenerative procedures [26, 35, 36], it has also been utilized to assess bone changes in peri-implantitis, in both preclinical and clinical investigations [27, 33, 37]. These studies, similar to the present investigation, reported an altered morphology of the peri-implant bone and a significant three-dimensional bone to implant contact (BIC) loss after ligature-induced peri-implantitis.

The use of optical scanners to superimpose and analyze virtual stereolithographic (STL) models has also been used reliably to evaluate the soft tissue volumetric and contour linear changes, in both preclinical and clinical investigations [25, 26, 38–41]. The present investigation, however, is the first time to use this technology to assess these changes in experimental peri-implantitis. Recently, a similar methodology was used in a human study to assess the volumetric changes after a bone regenerative intervention of peri-implantitis lesions [42]. In this study, STL files were obtained before

the regenerative procedure, and after 1 and 6 months. The results showed that peri-implant soft tissues underwent significant volumetric changes during all the different time points, especially at the marginal region.

As any preclinical *in vivo* study, this investigation has important limitations in regard to its possible translation of the obtained results to patients. Similarly, the limited sample size as a consequence to the need of reducing the number of experimental animals may limit the validity of the results. The experimental peri-implantitis model used in this investigation using submarginally placed ligatures exerts a mechanical effect superimposed to the chronic inflammation resulting from biofilm accumulation and this effect will not occur in the naturally developed disease. Furthermore, some methodological limitations related to the used method to analyze both the soft and hard tissue contours need to be mentioned. For an accurate record of the soft tissue profiles, the impressions need to be very precise and accurate, containing all the anatomical details. Hence, not all implants were analyzed in this investigation, but only those with precise recordings. However, with this selected material, the use of the presented method demonstrated a high degree of precision, with a measurement error below 20  $\mu$ m, and an excellent reproducibility with coefficients of variation ranging from 0.05 to 0.5% [43, 44]. The  $\mu$ CT analysis method used has the main limitation that soft tissue changes are not assessed, what implies the use of different methodological tools to assess the hard and the soft tissues. Finally, the lack of histological results in this report may limit a true understanding of the tissue behavior during the different phases of peri-implantitis.

## Conclusion

Within these limitations of this preclinical investigation, the results of this study evaluating the hard volumetric and soft tissue contour changes did not confirm that implants treated with a monolayer of multi-phosphonate molecules provided a more resistant environment to the pathological changes occurring in ligature-induced peri-implantitis. Therefore, future investigations are needed to confirm whether the addition to this implant surface provides a significant additional value to long-standing dental implant osseointegration.

**Supplementary Information** The online version contains supplementary material available at <https://doi.org/10.1007/s00784-020-03720-8>.

**Acknowledgments** The authors would like to express their gratitude to Liebert Parreiras Nogueira at the Clinical Oral Research Laboratory, Faculty of Dentistry, University of Oslo for their help preparing and analyzing the microCT data.

**Funding** This study was partially supported with a research contract between the University Complutense of Madrid and MIS Dental Implants.

## Compliance with ethical standards

**Conflict of interest** The authors declare that they have no conflict of interest.

**Ethical approval** AE-LU-001/04/16.

**Informed consent** For this type of study, formal consent is not required.

## References

- Moraschini V, da C Poubel LA, Ferreira VF, dos S P Barboza E (2015) Evaluation of survival and success rates of dental implants reported in longitudinal studies with a follow-up period of at least 10 years: a systematic review. *Int J Oral Maxillofac Surg* 44:377–388
- Pjetursson BE, Asgeirsson AG, Zwahlen M, Salier I (2014) Improvements in implant dentistry over the last decade: comparison of survival and complication rates in older and newer publications. *Int J Oral Maxillofac Implants* 29(suppl):308–324
- Caton J, Armitage G, Berglundh T et al (2018) A new classification scheme for periodontal and peri-implant diseases and conditions – introduction and key changes from the 1999 classification. *J Clin Periodontol* 45(Suppl 20):S1–S8
- Berglundh T, Armitage G, Araujo MG, Avila-Ortiz G, Blanco J, Camargo PM, Chen S, Cochran D, Derks J, Figuero E, Hämmeler CHF, Heitz-Mayfield LJA, Huynh-Ba G, Iacono V, Koo KT, Lambert F, McCauley L, Quirynen M, Renvert S, Salvi GE, Schwarz F, Tarnow D, Tomasi C, Wang HL, Zitzmann N (2018) Peri-implant diseases and conditions: consensus report of workgroup 4 of the 2017 World Workshop on the classification of periodontal and peri-implant diseases and conditions. *J Clin Periodontol* 45(Suppl 20):S286–S291
- Schwarz F, Derks J, Monje A, Wang HL (2018) Peri-implantitis. *J Clin Periodontol* 45(Suppl 20):S246–S266
- Derks J, Tomasi C (2015) Peri-implant health and disease. A systematic review of current epidemiology. *J Clin Periodontol* 42(Suppl. 16):S158–S171
- Krebs M, Kesar N, Begic A, von Krockow N, Nentwig G-H, Weigl P (2019) Incidence and prevalence of peri-implantitis and peri-implant mucositis 17 to 23 (18.9) years postimplant placement. *Clin Implant Dent Relat Res* 21:1116–1123. <https://doi.org/10.1111/cid.12848>
- Renvert S, Persson GR, Pirih FQ, Camargo PM (2018) Peri-implant health, peri-implant mucositis, and peri-implantitis: case definitions and diagnostic considerations. *J Clin Periodontol* 45(Suppl 20):S278–S285
- Ivanosky S, Lee R (2017) Comparison of peri-implant and periodontal marginal soft tissues in health and disease. *Periodontol* 0: 1–15
- Giovannoli JL, Rocuzzo M, Albouy JP, Duffau F, Lin GH, Serino G (2019) Local risk indicators - consensus report of working group 2. *Intern Dent J* 69(Suppl):7–11
- Dreyer H, Grischke J, Tiede C et al (2018) Epidemiology and risk factors of peri-implantitis: a systematic review. *J Periodontol* 00:1–25
- Saulaci N, Schaller B (2019) Prevalence of peri-implantitis in implants with turned and rough surfaces: a systematic review. *J Oral Maxillofac Res* 10(e1):1–12
- Jordana F, Susbielles L, Colat-Parros J (2018) Periimplantitis and implant body roughness: a systematic review of literature. *Implant Dent* 27(6):672–681
- Asensio G, Vazquez-Lasa B, Rojo L (2019) Achievements in the topographic design of commercial titanium dental implants: towards anti-peri-implantitis surfaces. *J Clin Med* 8(11):1982–2000
- Jansen JA, Brugge P, Van Der Waal E, Vredenberg A, Wolke J (2003) Osteocapacities of calcium phosphate ceramics. In: Ellingsen JE, Lyngstadaas SP (eds) *Bioimplant inter- face*. CRC, Boca Raton, pp 305–322
- Junker R, Dimakis A, Thoneick M, Jansen JA (2009) Effects of implant surface coatings and composition on bone integration: a systematic review. *Clin Oral Implants Res* 20(Suppl. 4):185–206
- Vionnery C, Chevolut Y, Léonard D, Aronsson BO, Péchy P, Mathieu HJ, Descouts P, Grätzel M (2002) Surface modification of titanium with phosphonic acid to improve bone bonding: characterization by XPS and ToF-SIMS. *Langmuir* 18:2582–2589
- Vionnery C, Guenther HL, Aronsson BO, Péchy P, Descouts P, Grätzel M (2002) Osteoblast culture on polished titanium disks modified with phosphonic acids. *J Biomed Mater Res* 62:149–155
- Von Salis-Soglio M, Stübinger S, Sidler M, Klein K, Ferguson S, Kämpf K et al (2014) A novel multi-phosphonate surface treatment of titanium dental implants: a study in sheep. *J Funct Biomater* 5(3): 135–157
- Esposito M, Dojcinovic I, Germon L, Lévy N, Curno R, Buchini S, Péchy P, Aronsson BO (2013) Safety and efficacy of a biomimetic monolayer of permanently bound multi-phosphonic acid molecules on dental implants: 1year post-loading results from a pilot quadruple-blinded randomised controlled trial. *Eur J Oral Implantol* 6:227–236
- Vignoletti F, Abrahamsson I (2012) Quality of reporting of experimental research in implant dentistry. Critical aspects in design, outcome assessment and model validation. *J Clin Periodontol* 39(Suppl. 12):6–27
- Lindhe J, Berglundh T, Ericsson I, Liljenberg B, Marinello C (1992) Experimental breakdown of peri-implant and periodontal tissues. A study in the beagle dog. *Clin Oral Implants Res* 3(1):9–16
- Feldkamp LA, Davis LC, Kress JW (1984) Practical cone-beam algorithm. *J Opt Soc Am* 1(6):612–619
- Becker K, Wilmes B, Grandjean C, Drescher D (2018) Impact of manual control point selection accuracy on automated surface matching of digital dental models. *Clin Oral Investig* 22(2):801–810
- Di Raimondo R, Sanz-Esporrin J, Pla R, Sanz-Martin I, Luengo F, Vignoletti F, Nuñez J, Sanz M (2020) Alveolar crests contour changes after guided bone regeneration using different biomaterials: an experimental in vivo investigation. *Clin Oral Investig* 24(7):2351–2361
- Di Raimondo R, Sanz-Esporrin J, Sanz-Martin I, Pla R, Luengo F, Vignoletti F, Nuñez J, Sanz M (2020) Hard and soft tissue changes after guided bone regeneration using two different barrier membranes: an experimental in vivo investigation. *Clin Oral Investig*. <https://doi.org/10.1007/s00784-020-03537-5>
- Godoy-Gallardo M, Manzanares-Cespedes MC, Sevilla P, Nart J, Manzanares N, Manera JM, Gil FJ, Body SK, Rodriguez D (2016) Evaluation of bone loss in antibacterial coated dental implants: an experimental study in dogs. *Mater Sci Eng C Mater Biol Appl* 69: 538–545
- Berglundh T, Gotfredsen K, Zitzmann NU, Lang NP, Lindhe J (2007) Spontaneous progression of ligature induced peri-implantitis at implants with different surface roughness: an experimental study in dogs. *Clin Oral Implants Res* 18:655–661
- Albouy JP, Abrahamsson I, Persson LG, Berglundh T (2008) Spontaneous progression of peri-implantitis at different types of implants. An experimental study in dogs. I: clinical and radiographic observations. *Clin Oral Implants Res* 19(10):997–1002
- Albouy JP, Abrahamsson I, Persson LG, Berglundh T (2009) Spontaneous progression of ligature induced peri-implantitis at

- implants with different surface characteristics. An experimental study in dogs II: histological observations. *Clin Oral Implants Res* 20(4):366–371
31. Fickl S, Kerschull M, Calvo-Guirado JL, Hurzeler M, Zuhr O (2015) Experimental peri-implantitis around different types of implants – a clinical and radiographic study in dogs. *Clin Implant Dent Relat Res* 17(Suppl 2):e661–e669
  32. Sanz-Esporrin J, Blanco J, Sanz-Casado JV, Muñoz F, Sanz M (2019) The adjunctive effect of rhBMP-2 on the regeneration of peri-implant bone defects after experimental peri-implantitis. *Clin Oral Implants Res* 30(12):1209–1219
  33. Maglione M, Vaccari L, Mancini L, Ciancio R, Bedolla DE, Bevilacqua L, Tonellato P (2019) Micro-ATR FTIR, SEM-EDS and X-ray micro-CT: an innovative multi-technique approach to investigate bone affected by peri-implantitis. *Int J Oral Maxillofac Implants* 34(3):631–641
  34. Finelle G, Papadimitriou DEV, Souza AB, Katebi N, Gallucci GO, Araujo MG (2015) Peri-implant soft tissue and marginal bone adaptation on implant with non-matching healing abutments: micro-CT analysis. *Clin Oral Implants Res* 26:e42–e46
  35. Thoma DS, Jung U-W, Park J-Y, Bienz SP, Husler J, Jung RE (2017) Bone augmentation at peri-implant dehiscence defects comparing a synthetic polyethylene glycol hydrogel matrix versus standard guided bone regeneration techniques. *Clin Oral Implants Res* 28:e76–e83
  36. Khobragade P, Jain A, Setlur Nagesh SV, Andreana S, Dziak R, Sunkara SK, Ionita CN (2015) Micro-computed tomography (CT) based assessment of dental regenerative therapy in the canine mandible model. *Proc SPIE Int Soc Opt Eng* 17:9417
  37. Qian W, Qiu J, Liu X (2019) Minocycline hydrochloride loaded graphene oxide films on implant abutments for peri-implantitis treatment in beagle dogs. *J Periodontol* 91:792–799. <https://doi.org/10.1002/JPER.19-0285>
  38. Sanz-Martin I, Benic GI, Hammerle CH, Thoma DS (2016) Prospective randomized controlled clinical study comparing two dental implant types: volumetric soft tissue changes at 1 year of loading. *Clin Oral Implants Res* 27:406–411
  39. Sanz-Martin I, Vignoletti F, Nuñez J, Permuy M, Muñoz F, Sanz-Esporrin J, Fierravanti L, Shapira L, Sanz M (2017) Hard and soft tissue integration of immediate and delayed implants with a modified coronal macro design: histological, micro CT and volumetric soft tissue changes from a pre-clinical in vivo study. *J Clin Periodontol* 44(8):842–853
  40. Sanz-Martin I, Ferrantino L, Vignoletti F, Nunez J, Baldini N, Duvina M, Alcaraz J, Sanz M (2018) Contour changes after guided bone regeneration of large non-contained mandibular buccal bone defects using deproteinized bovine bone mineral and a porcine-derived collagen membrane: an experimental in vivo investigation. *Clin Oral Investig* 22(3):1273–1283
  41. Basler T, Naenni N, Schneider D, Hammerle CHF, Jung R, Thoma DS (2018) Randomized controlled clinical study assessing two membranes for guided bone regeneration of peri-implant bone defects: 3-year results. *Clin Oral Implants Res* 29(5):499–507
  42. Galarraga-Vinueza ME, Obreja K, Magini R, Sculean A, Sader R, Schwarz F (2020) Volumetric assessment of tissue changes following combined surgical therapy of peri-implantitis: a pilot study. *J Clin Periodontol* 00:1–10. <https://doi.org/10.1111/jcpe.13335>
  43. Mehl A, Gloger W, Kunzelmann KH, Hickel R (1997) A new optical 3-D device for the detection of wear. *J Dent Res* 76(11):1799–1807
  44. Windisch SI, Jung RE, Sailer I, Studer SP, Ender A, Hämmerle CHF (2007) A new optical method to evaluate three-dimensional volume changes of alveolar contours: a methodological in vitro study. *Clin Oral Implants Res* 18:545–551

**Publisher's note** Springer Nature remains neutral with regard to jurisdictional claims in published maps and institutional affiliations.